Supplemental Materials

Molecular Biology of the Cell

Baumhardt *et al*.

Supplemental Tables

Supplemental Table 1. Data collection and refinement statistics for WT CRM1 structures.

Data collection						
WT CRM1*-Ran-RanBP1 bound to:	Mek1^{NES}	4E-T^{NES}	Mek1 NQ^{NES}	PKI^{NES}	PKI DE^{NES}	Unliganded
Space group	$P4_32_12$					
Cell dimensions a=b, c (Å)	106.9, 303.9	106.6, 303.7	106.9, 303.4	106.7, 303.5	107.2, 305.1	105.3, 306.7
Resolution range (Å)	50.00-2.40 (2.44-2.40)	50.00-2.30 (2.34-2.30)	50.00-2.50 (2.54-2.50)	50.00-2.20 (2.24-2.20)	50.00-2.86 (2.91-2.86)	49.80-2.35 (2.39-2.35)
Multiplicity	26.0 (26.8)	15.8 (14.4)	18.1 (15.3)	21.6 (21.8)	16.6 (16.4)	7.2 (7.2)
Completeness (%)	100 (100)	99.9 (99.9)	99.9 (99.8)	99.9 (99.9)	100 (100)	99.9 (99.9)
R_{meas} /R_{pim} (%)	15.7/5.0 (0/58.4)	16.5/4.0 (342.3/84.5)	15.0/3.5 (227.0/56.0)	58.9/13.3 (0/351.0)	40.0/10.6 (0/255.8)	9.2/3.4 (206.7/76.2)
I/σ(I)	33.1 (3)	23.5 (1.1)	25.2 (1.8)	26.1 (1.4)	20.75 (1.6)	22.1 (1.0)
$CC_{1/2}$ (last resolution shell)[a]	0.80	0.50	0.59	0.50	0.45	0.59
Refinement statistics						
Resolution range (Å)	40.47-2.40 (2.46-2.40)	42.02-2.30 (2.36-2.30)	47.32-2.50 (2.56-2.50)	47.30-2.20 (2.23-2.20)	47.96-2.82 (2.89-2.82)	37.23-2.35 (2.39-2.35)
# reflections R_{work}/R_{free}	5205/154 (4604/136)	5877/154 (5279/136)	4631/158 (2973/102)	7167/175 (1794/43)	3243/166 (1217/62)	6153/215 (880/30)
Data completeness (%)	100 (97)	100 (98)	100 (71)	82 (25)	93 (42)	64 (14)
Atoms (non-H protein/ solvent)	10944/492	10914/170	10957/341	10865/693	10912/0	11072/138
R_{work}/R_{free}(%)	21.1/25.2 (27.8/36.1)	22.3/25.7 (31.6/36.7)	19.8/24.6 (26.5/35.8)	20.8/24.0 (30.8/38.9)	20.6/26.2 (29.9/43.2)	23.3/26.1 (31.6/51.8)
R.m.s.d. Bond length (Å) /angle (°)	0.003/0.5	0.005/0.7	0.003/0.6	0.003/0.6	0.003/0.5	0.003/0.5
Mean B-value (Å^2)	34.0	50.7	34.3	28.3	44.9	30.0
Ramachandran plot favored /disallowed(%)[b]	97.8/0.1	97.8/0.1	97.8/0.1	98.1/0.1	96.4/0.2	96.2/0.6
ML coordinate error	0.29	0.32	0.32	0.26	0.35	0.24
PDB code	6X2P	6X2R	6X2S	6X2U	6X2V	6X2M

Data for the outermost shell are in parentheses.

[a] Karplus PA & Diederichs K (2012) Linking crystallographic model and data quality. Science 336(6084):1030-1033.

[b] As defined by MolProbity in PHENIX.

Supplemental Table 2. Data collection and refinement statistics for CRM1(E571K) structures

Crystal of CRM1(E571K)*-Ran-RanBP1 bound to:	PKI^{NES}	Mek1^{NES}	mDia2^{NES}	Unliganded
Space group	$P4_32_12$			
Cell dimensions a=b, c (Å)	106.6, 302.7	106.7, 303.8	106.7, 304.0	105.3, 306.5
Resolution range (Å)	50.00 -3.00 (3.05-3.00)	50.00-2.45 (2.49-2.45)	50.00-2.30 (2.34-2.30)	50.00-2.55 (2.59-2.55)
Multiplicity	7.6 (5.6)	34.5 (29.8)	20.6 (19.0)	7.2 (7.5)
Data completeness (%)	93 (95)	99 (86)	100 (100)	100 (100)
R_{meas} /R_{pim} (%)	22.5/7.8 (133.2/54.8)	9.8/1.9 (0/30.2)	32.7/7.1 (381.3/86.1)	20.9/7.8 (187.3/68.2)
I/σ(I)	13.5 (1.8)	42 (2.5)	25 (1.5)	12.3 (1.3)
$CC_{1/2}$ (last resolution shell)[a]	0.54	0.3	0.56	0.54
Refinement statistics				
Resolution range (Å)	47.13-7.22 (3.07-3.00)	40.21-2.46 (2.52-2.46)	45.78-2.30 (2.34-2.30)	43.39-2.55 (2.61-2.55)
No. of reflections R_{work}/R_{free}	2330/154 (1793/118)	4820/154 (4089/131)	6526/183 (1404/39)	4226/165 (1958/76)
Data completeness (%)	90 (76)	99 (93)	77 (21)	99 (50)
Atoms (non-H protein/solvent)	10901/0	11454/476	11360/466	11000/296
R_{work}/R_{free} (%)	20.0/25.3 (31.8/37.7)	20.2/25.0 (23.7/29.9)	20.5/25.6 (33.4/46.6)	22.2/25.4 (28.2/28.4)
R.m.s.d. Bond length (Å)/angle (°)	0.003/0.5	0.005/0.7	0.003/0.5	0.004/0.6
Mean B-value (Å^2)	56.0	33.0	29.2	39.5
Ramachandran plot favored /disallowed (%)[b]	95.4/0.15	97.37/0.08	97.73/0.08	97.52/0.08
ML coordinate error	0.36	0.30	0.29	0.31
PDB code	6X2W	6X2X	6X2Y	6X2O

Data for the outermost shell are given in parentheses.

[a] Karplus PA & Diederichs K (2012) Linking crystallographic model and data quality. Science 336(6084):1030-1033.

[b] As defined by MolProbity in PHENIX.

Supplemental Table 3. The list of putative NESs with charged β-strands obtained from structure-based NES prediction.

[Excel File Download]

Supplemental Table 4. Chronic Lymphocytic Leukemia patient samples. Information on cytogenetics, age, and treatment information of patient samples immunostained for 4E-T.

Patient ID	XPO1 Genotype	Cytogenetics	Age	Treatment
WT-1	WT	del(11q), del(13q)	60	lenalidomide
WT-2	WT	del(11q), del(13q)	56	-
WT-3	WT	del(13q)	54	-
WT-4	WT	del(11q)	69	ofatumumab
WT-5	WT	normal	63	-
K-1	E571K	del(13q)	85	-
K-2	E571K	del(13q)	74	-
K-3	E571K	del(11q), del(13q)	67	ibrutinib
K-4	E571K	del(13q), +2p12-13(REL)*	38	-
K-5	E571K	normal	46	-

*****No duplication of CRM1 was observed as a result of the +2p12-13 event

Supplemental Table 5. NES peptide sequences cloned into pMAL-TEV for binding affinity measurements.

Cargo Protein	NES Sequence
Mek1	TNLEALQKKLEELELDEQ
P73	NFEILMKLKESLELMELVP
hRio2	RSFEMTEFNQALEEIKG
X11L2	SSLQELVQQFEALPGDLV
mDia2	SVPEVEALLARLRAL
Iκβα	EQMVKELQEIRLEPQ
Snupn1	MEELSQALASSFSVSQDLNS
HIV Rev	LQLPPLERLTLDC
Smad4	YERVVSPGIDLSGLTLQ
FMRP1b	LKEVDQLRALERLQID
Dusp6	PLPVLGLGGLRISS
Cpeb4	RTFDMHSLESSIDIMR
Iκβε	SLVLLPFDDLKISG
Paxillin	RELDELMASLSDFKFMA
PKI	NSNELALKLAGLDINK
PP2A B56α	REELWKKLEELKLKK
eIF4E-Transporter	SVEEVEAGLKGLKVDQQVK
RPS2	DKEWMPVTKLGRLVKDMKIKS
KATNAL1	EQVKSIVSTLESFKIDK
PARVG	DGLILHHLFQRLAALKLEAED
ING3	DRHLRKLDQELAKFKMELADN
NUP62	EKITSLHREVEKVKLDQKR
KIF5A	QHEAKIRSLTEYMQSVELKKR
BAZ1A	KENGIIKTVNEDVEEMEIDEQ
SIKE1	DDQFCKIQEKLAQLELENK
CPE290	DREIEILTKEINKLELKISD
COPB2	EKSLLELEVDLDNLELED

Supplemental Figures

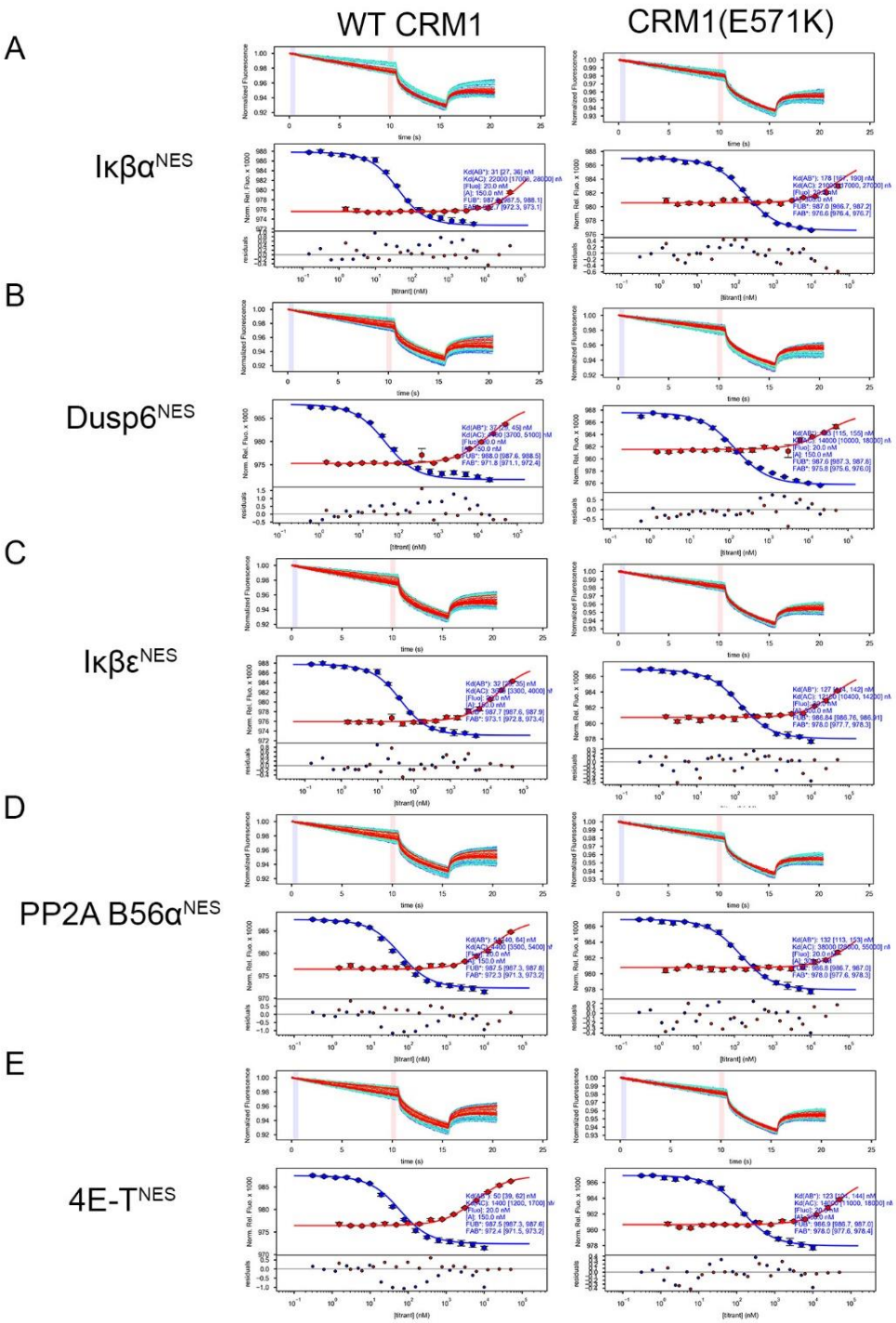

Supplemental Figure 1. NESs with charged β-strands binding to WT CRM1 or CRM1(E571K)**.** Raw binding affinity isotherms from differential photobleaching assays (performed in triplicate) for NES peptides binding to WT CRM1 and to CRM1(E571K).

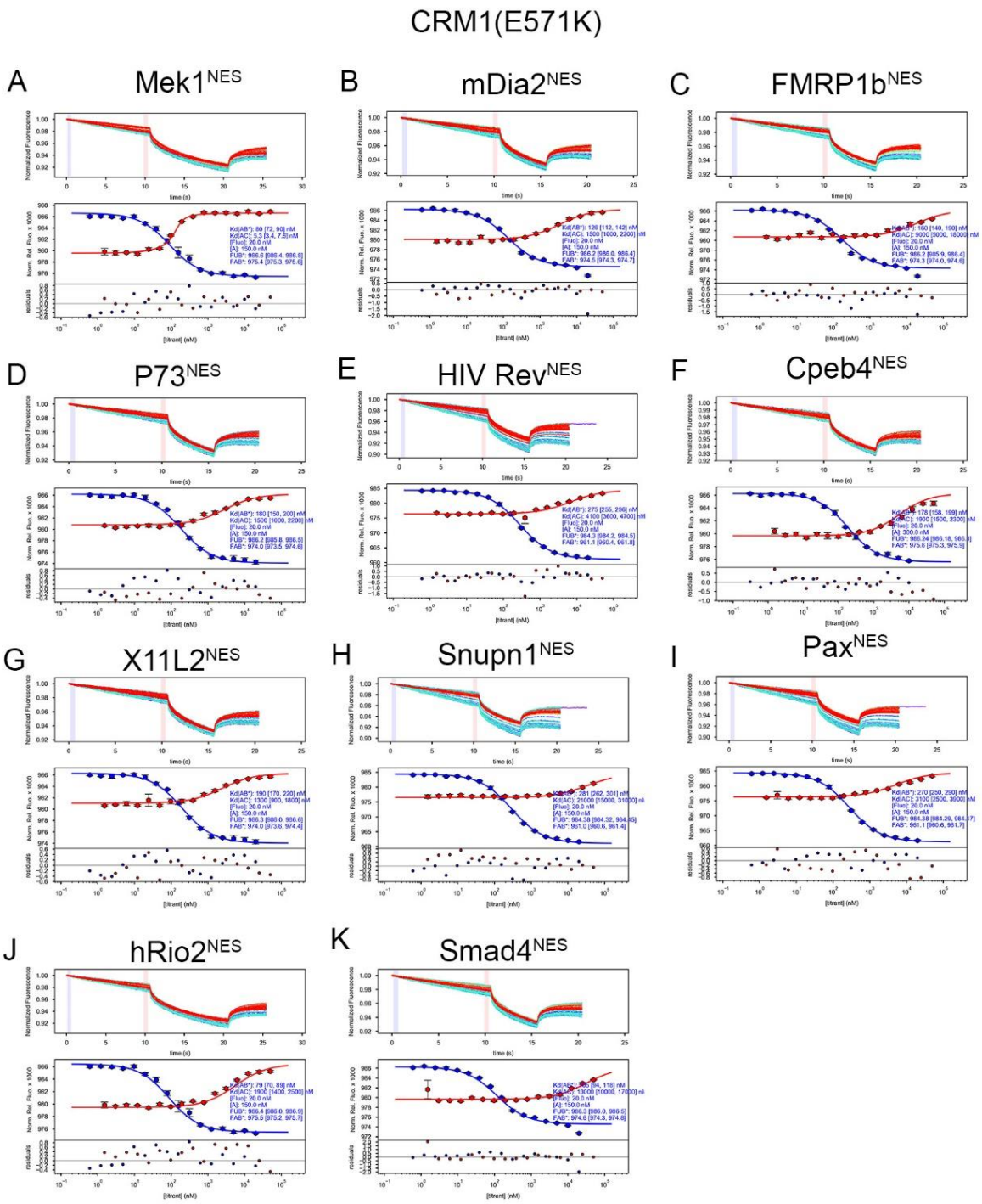

Supplemental Figure 2. CRM1(E571K) binding to NES peptides. Raw binding affinity isotherms from differential photobleaching assays (performed in triplicate) for NESs binding to CRM1(E571K). Binding affinities of these peptides for WT CRM1 were previously reported in [11,14].

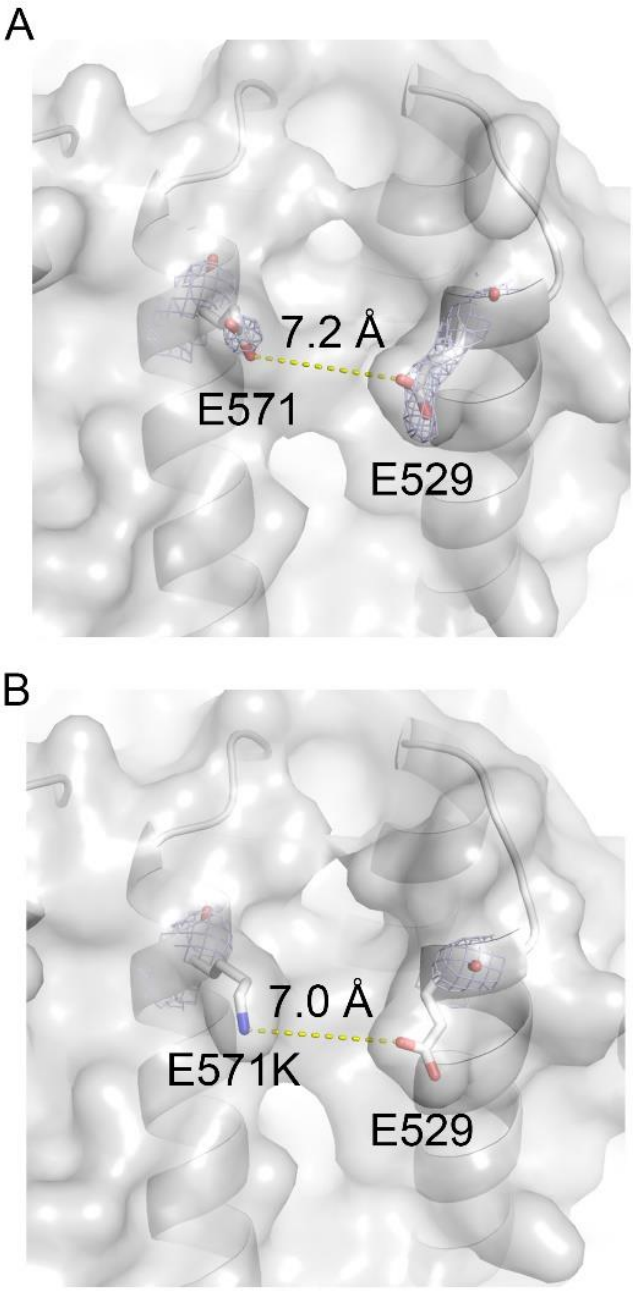

Supplemental Figure 3. Structures of unliganded WT CRM1 and CRM1(E571K). Surface representations of the closed NES grooves of unliganded WT CRM1 (A) and unliganded CRM1(E571K) (B) showing the side chains of position 571 pointing toward solvent and located far from the helix of HEAT repeat 11 on the other side of the groove. Electron densities (from $2F_o$-F_c composite omit map, contoured at 1σ) for side chains of position 571 are drawn as a blue mesh.

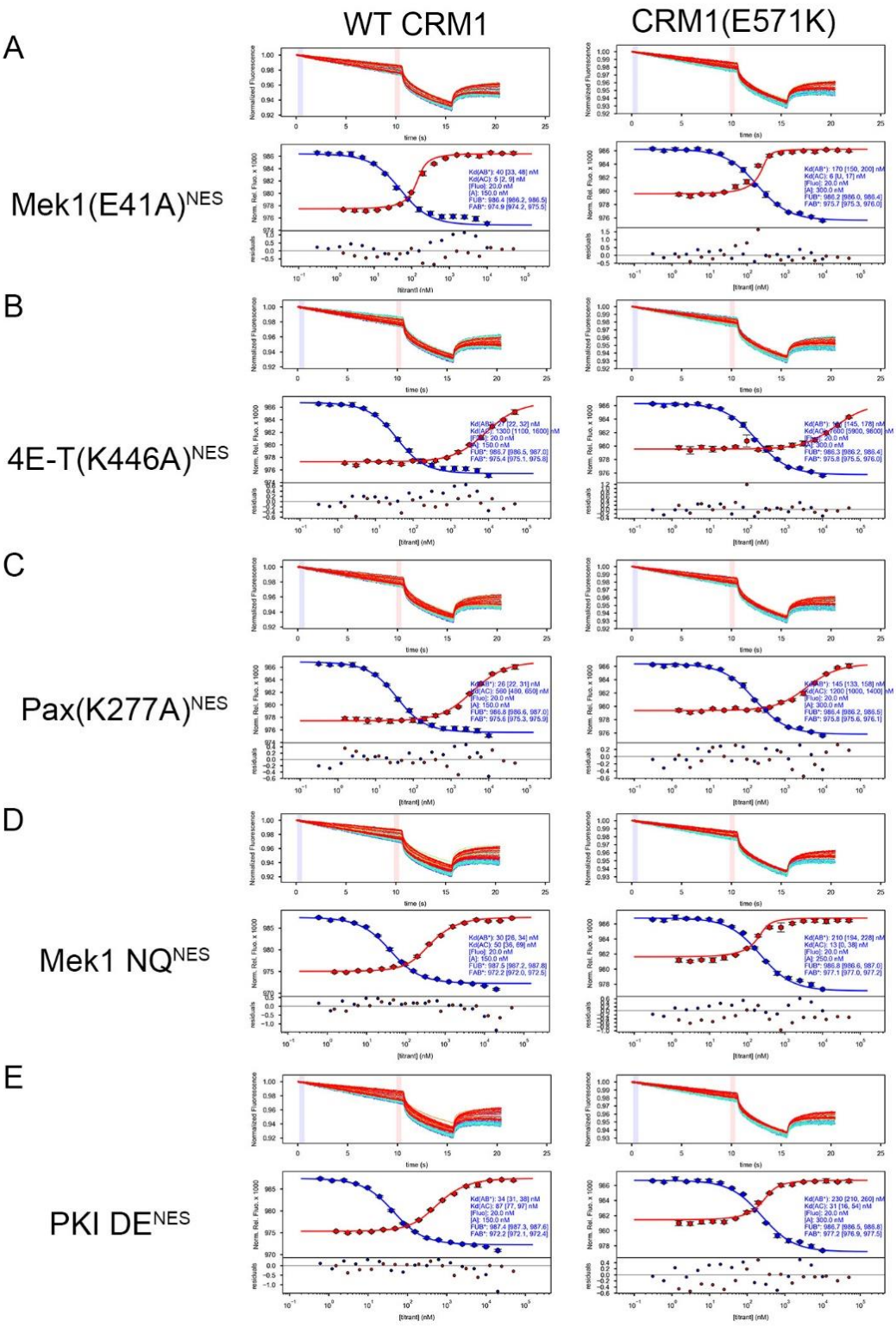

Supplemental Figure 4. WT CRM1 and CRM1(E571K) binding to mutated NES peptides. Raw binding affinity isotherms from differential photobleaching assays (performed in triplicate) for mutated NES peptides binding to WT CRM1 and CRM1(E571K).

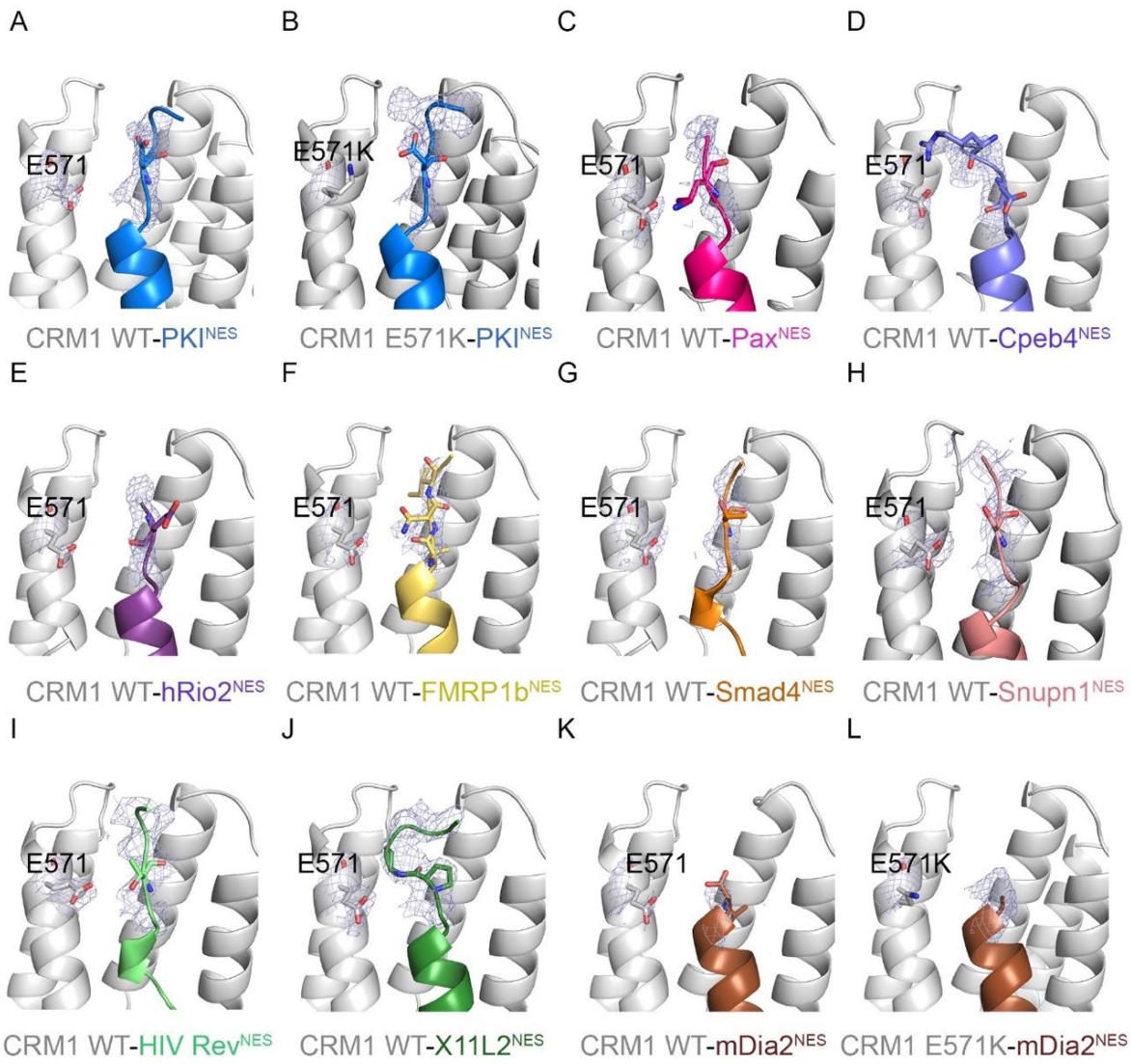

Supplemental Figure 5. Structures of CRM1-bound NESs that have modest or no binding affinity differences for WT vs. E571K CRM1. (A) Structure of PKI^{NES} (blue) bound to WT CRM1 (grey) (B) Structure of PKI^{NES} (blue) bound to CRM1(E571K) (grey). (C-J) Structures of WT CRM1 (grey) bound to the Pax^{NES} (pink, PDB 5UWH; C), Cpeb4^{NES} (light purple, PDB 5DIF; D), hRio2^{NES} (dark purple, PDB 5DHF; E) FMRP1b^{NES} (gold, PDB 5UWO; F), Smad4^{NES} (orange, PDB 5UWU; G), Snupn1^{NES} (peach, PDB 3GJX; H), HIV Rev^{NES} (light green, PDB 3NBZ; I), X11L2^{NES} (moss green, PDB 5UWS; J). (K-L) Structure of mDia2^{NES} (bronze) bound to WT CRM1 (grey, PDB 5UWP; K) and to CRM1(E571K) (grey; L).

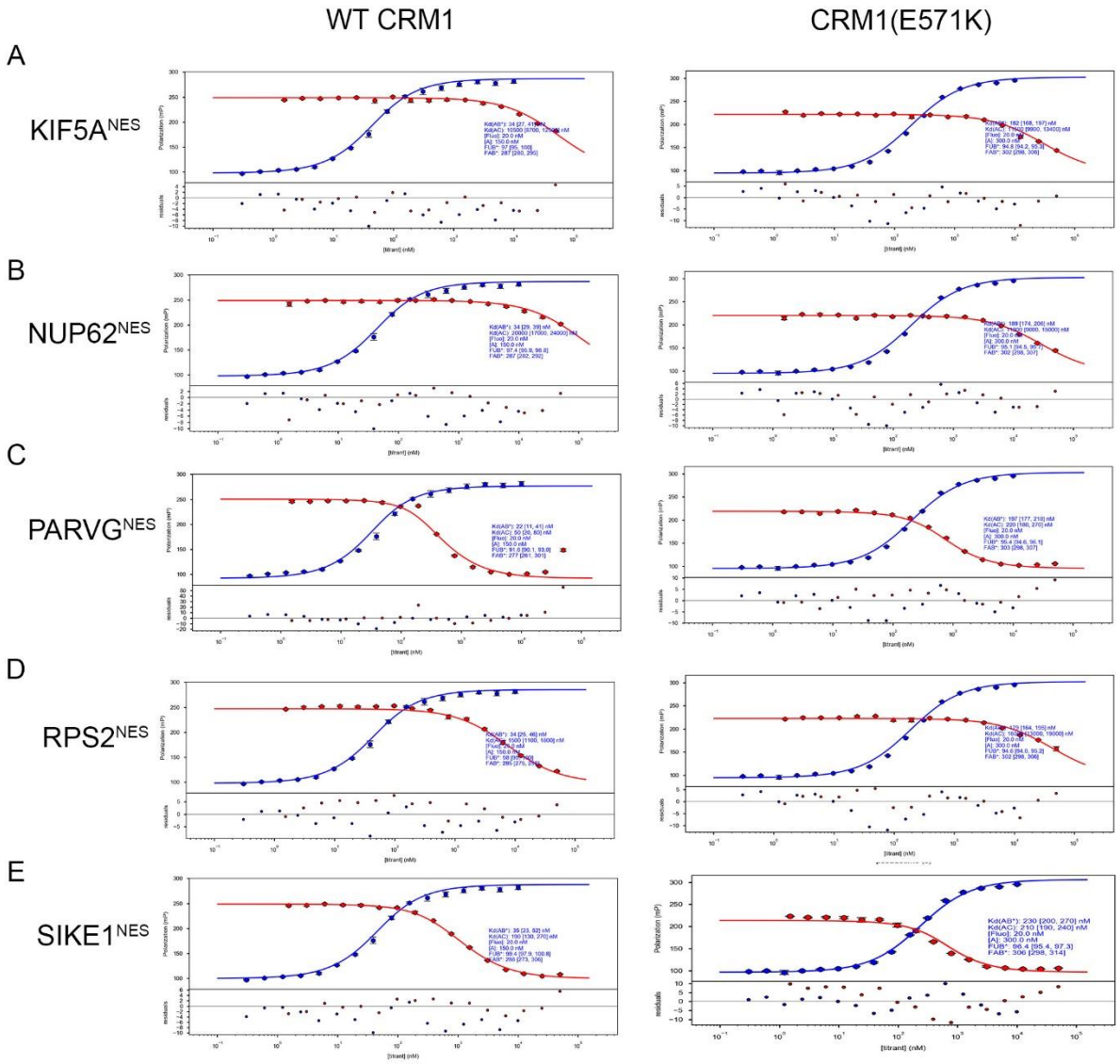

Supplemental Figure 6. WT CRM1 and CRM1(E571K) binding to putative NESs identified by structure-based NES prediction. Raw binding affinity isotherms from fluorescence polarization assays (performed in triplicate) of putative NES peptides binding to WT CRM1 and to CRM1(E571K).

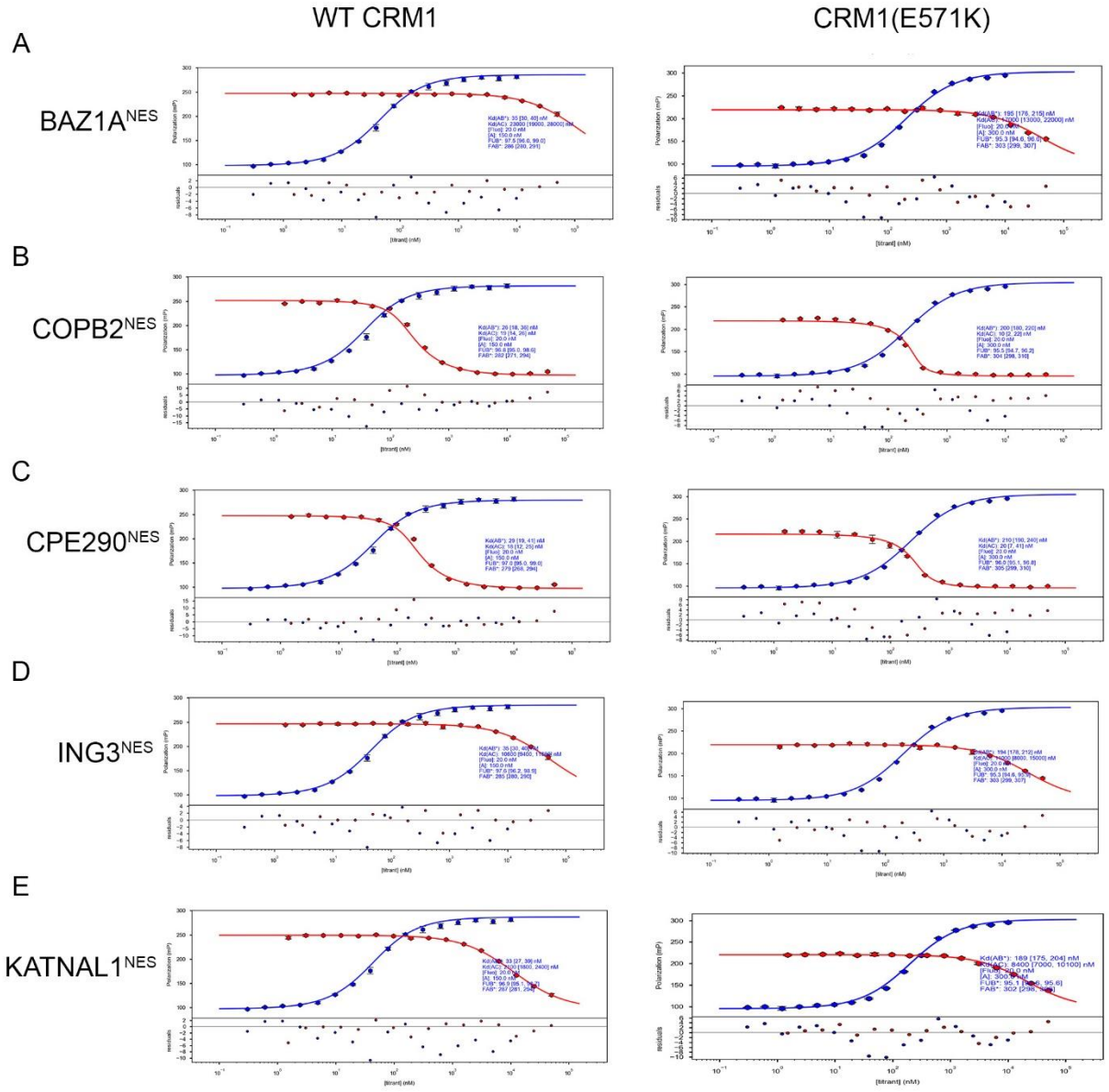

Supplemental Figure 7. WT CRM1 and CRM1(E571K) binding to another five putative NESs identified by structure-based NES prediction. Raw binding affinity isotherms from fluorescence polarization assays (performed in triplicate) of putative NES peptides binding to WT CRM1 and to CRM1(E571K).

A

Cargo	NES β-strand	Binding Affinity (K_D) WT CRM1	Binding Affinity (K_D) CRM1(E571K)	K_D,E571K/ K_D,WT
eIF4E-T	LKVDQ	1.4 μM [1.2-1.7 μM]	14 μM [11-18 μM]	10
Nup62	VKLDQ	20 μM [17-24 μM]	11 μM [9-15 μM]	0.6
Mek1	LELDE	70 nM [40-130 nM]	5 nM [3-8 nM]	0.071
BAZ1A	MEIDE	23 μM [19-28 μM]	17 μM [13-20 μM]	0.7

B

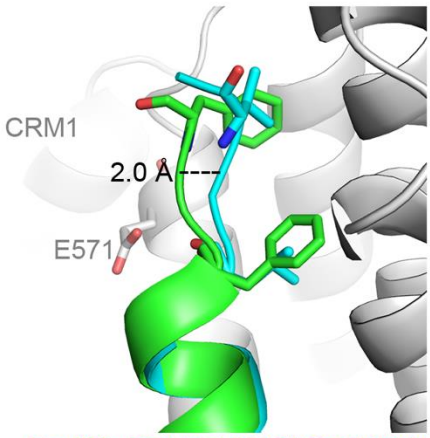

Supplemental Figure 8. Hydrophobic side chains in the NES β-strand affect binding to CRM1 E571K. (A) Information for NESs (4E-T^{NES}, Mek1^{NES}) or putative NESs (Nup62^{NES}, BAZ1A^{NES}). 4E-T^{NES} and Nup62^{NES} share the same X (positions between hydrophobic residues) side chains, ϕ3Kϕ4DQ, but bind differently to WT vs. E571K CRM1. Mek1^{NES} and BAZ1A^{NES} also share the same X side chains, ϕ3Eϕ4DE, and bind differently to WT vs. E571K CRM1. (B) The β-strand of Pax^{NES} (PDB: 5UWH, green), which has bulky aromatic ϕ3 and ϕ4 side chains, binds in the CRM1 groove quite differently from the β-strand 4E-T^{NES}, which has shorter aliphatic hydrophobic side chains. The different conformations place them at different distances from the Glu571 side chain of CRM1.

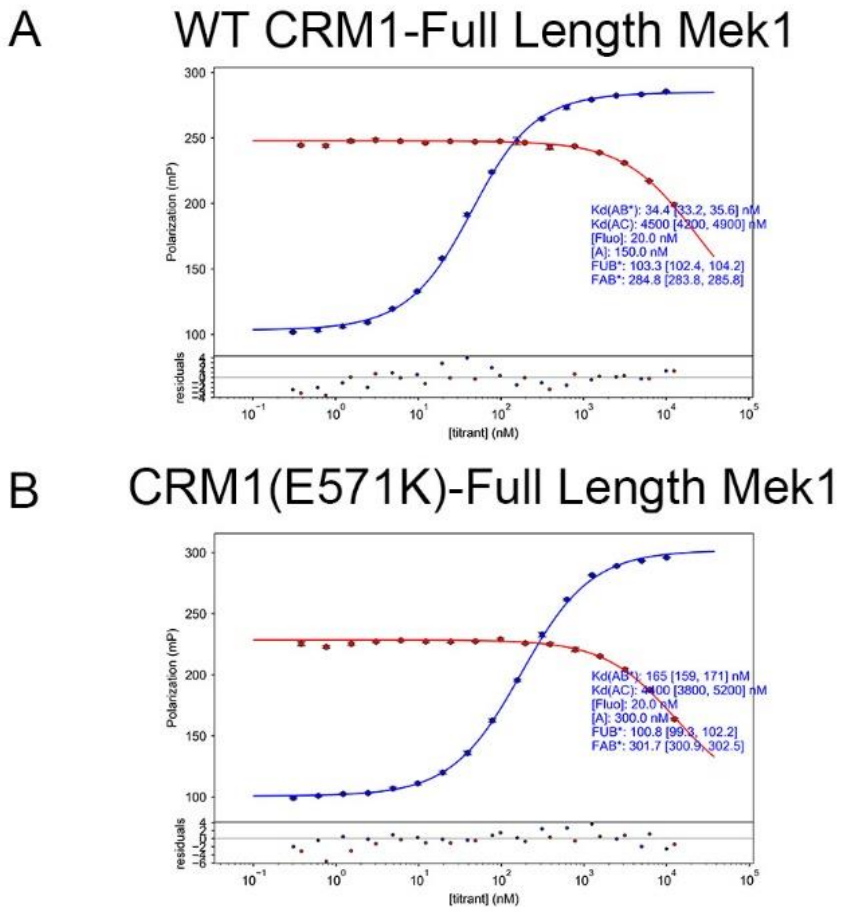

Supplemental Figure 9. Full length Mek1 binds similarly to WT CRM1 and CRM1(E571K). Raw binding affinity isotherms from fluorescence polarization assays (performed in triplicate) of full length Mek1 for WT CRM1 (A) and CRM1(E571K) (B).

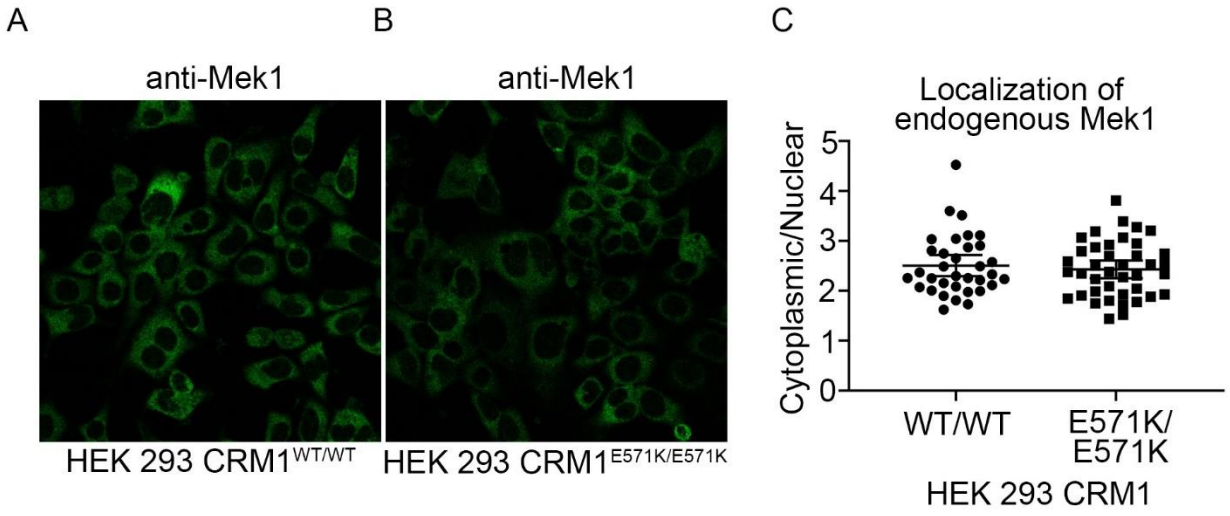

Supplemental Figure 10. Quantification of the cytoplasmic/nuclear ratio of endogenous Mek1 in HEK 293 cells. (A) Immunostain with anti-Mek1 and a fluorescently tagged secondary antibody of endogenous Mek1 in HEK 293 cells with WT CRM1 or (B) CRM1(E571K). (C) Quantification of the cytoplasmic/nuclear signal of Mek1.

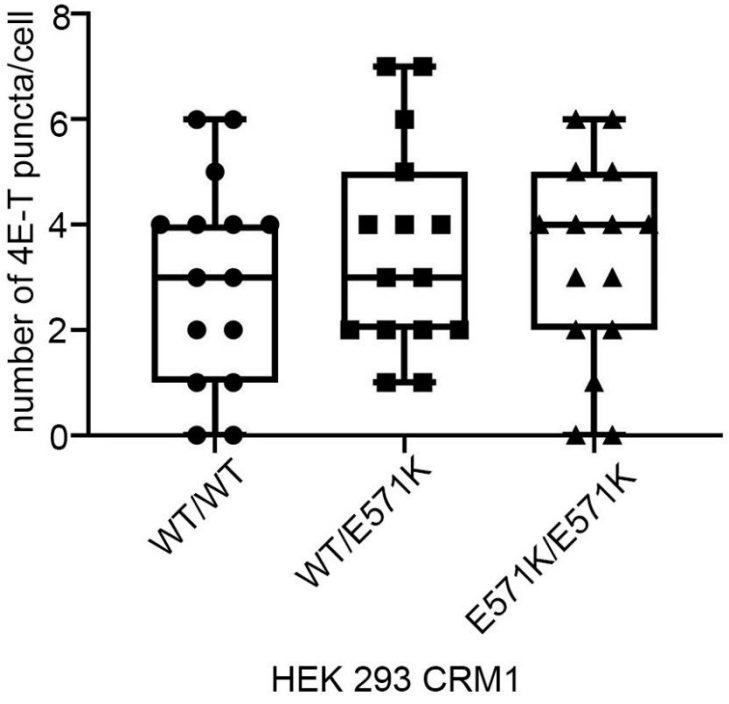

Supplemental Figure 11. Counting the 4E-T-containing cytoplasmic puncta in HEK 293 $CRM1^{WT/WT}$ $CRM1^{WT/E571K}$ and $CRM1^{E571K/E571K}$ cells. HEK 293 cells were immunostained using anti-4E-T antibody, and imaged using confocal microscopy. Image intensity threshold was set with ReyniEntropy at 60,000, and the number of puncta in each cell were counted manually.

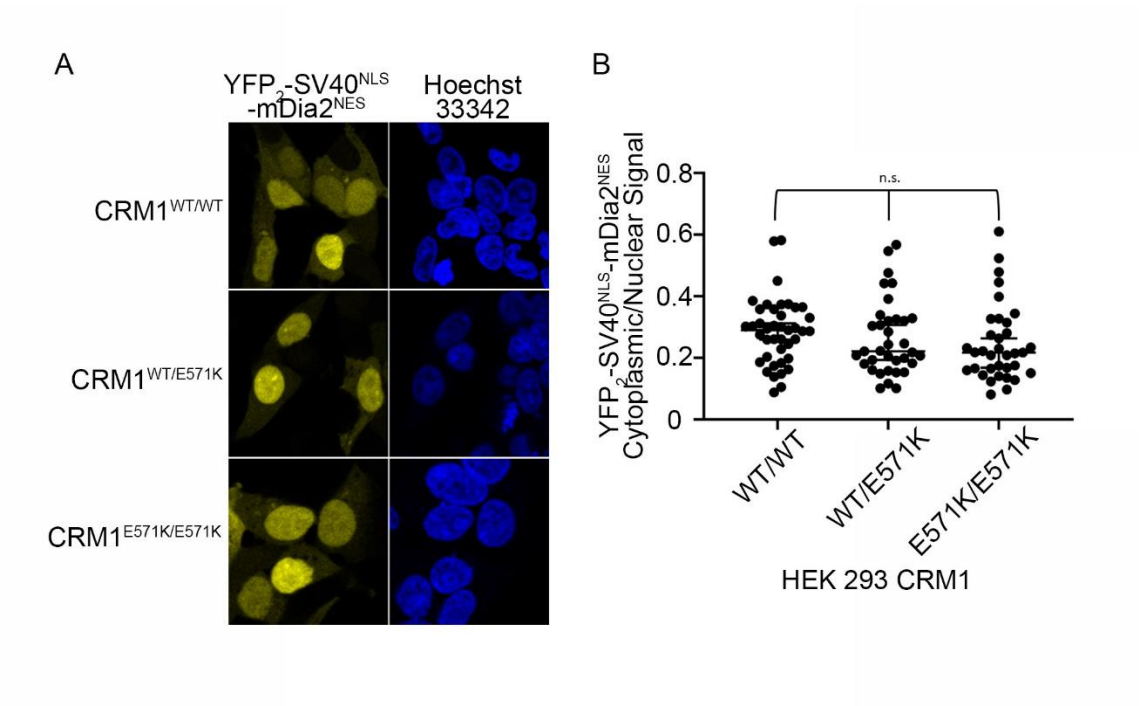

Supplemental Figure 12. Cytoplasmic-nuclear localization of YFP_2-$SV40^{NLS}$-$mDia2^{NES}$ in HEK 293 cells. (A) Confocal microscopy images of HEK 293 cells transiently transfected with the fluorescent reporter YFP_2-$SV40^{NLS}$-$mDia2^{NES}$. (B) Quantification of the cytoplasmic/nuclear ratio of the reporter signal.